Steps in gas-surface reactions

Lent, R. van

Chapter 5

Step-type dependence of oxygen reduction on Pt(1 1 1) surfaces

A model fully ascribes oxygen reduction reactivity on Pt(1 1 1) to a single unknown surface defect, but it disregards the influence of other types of surface defects. Some elementary reaction steps involved are sensitive to step type. Here, we confirm that step defect type indeed influences oxygen reduction by impinging two molecular beams onto two stepped Pt(1 1 1) surfaces containing different step types. The two molecular beams used consist of pure oxygen and a hydrogen-deuterium mixture respectively. Our results show that one step type, {1 1 0} step edges, is more reactive than {0 0 1} steps under oxygen lean reaction conditions. These results show that defect type is an important consideration in reactivity studies that consider the complete reaction mechanism.

Introduction

Fuels cells are a promising avenue for using renewable energy stored into chemical bonds. One of the biggest challenges in proton exchange membrane fuel cells is rate limiting oxygen reduction at the anode.[95] Reaction rates during catalysis depend on the reaction mechanisms at play, which are strongly influenced by the nature of the catalyst.[96, 97] One of the best catalysts for oxygen reduction is platinum. The current model[98] based on experimental results on Pt(1 1 1) suggests two overall mechanisms take place: sequential addition of H_{ads} at low temperature (T_s) and disproportionation of H_2O_2 that transports H_{ads} to the active site at elevated T_s. Eventual water formation is proposed to occur at one single reaction site by varying the defect density through sputtering. Although the model[98] for Pt(1 1 1) points toward defects as the active site, the nature of the active site remains unclear. The sputter approach offers little control in the types of defects present at the surface.[99]

Specific surface sites of catalysts may influence catalytic activity[47] and selectivity[100] of chemical reactions. Ample evidence shows that various elementary steps in oxygen reduction are structure sensitive as well. First, we showed in chapter 3 that dissociative adsorption of H_2 on stepped Pt surfaces exhibits higher reactivity at {1 1 0} (B-type) step edges than {0 0 1} (A-type) steps.[79] Second, O_2 sticking probabilities for the two step types differ with incident energy (E_{kin})[101, 102] and molecular orientation[27]. Third, desorption energies for hydrogen, oxygen, and water differ for the two step types.[51] Thermal desorption of co-adsorbed water and oxygen suggests that OH formation, the key intermediate to water formation, favors B-type steps over A-type.[103] These observations make it likely that water formation from hydrogen and oxygen is step type dependent as well.

Here, we investigate whether oxygen reduction is step-type dependent by reacting oxygen with a mixed H_2/D_2 beam on oxygen-covered Pt(3 3 5) and Pt(5 5 3) surfaces. B-type steps of Pt(5 5 3) exhibit significantly higher O_2 reaction probabilities than A-type steps of Pt(3 3 5) under similar

conditions despite having a lower step density. After O_{ads} depletion under hydrogen rich conditions, O_2 sticking probabilities (S) resemble the initial sticking probabilities (S_0) on the clean surface. Our results suggest that neither step-type requires significant θ_O to catalyze the reaction. Higher B-type sticking probabilities during the reaction show structure sensitivity for water formation.

Method

The experiment is schematically illustrated in figure 5.1. The Pt(3 3 5) and Pt(5 5 3) surfaces are precovered in O_{ads} using a supersonic molecular beam of O_2, depicted in red. Afterwards, a 1:1 mixed H_2:D_2 beam impinges the sample simultaneous to the O_2 beam. The incident H_2 and D_2 dissociate and subsequently react with O_{ads} to form water for 30 s. Subsequently, the O_2 beam flag is closed so that remaining O_{ads} is titrated by the hydrogen beam.

With the surfaces covered (but not saturated) with O_{ads}, they are subsequently exposed to both a supersonic O_2 and effusive hydrogen beam. The latter consists of equal amounts of H_2 and D_2. H_2 and D_2 dissociate and may either react with adsorbed oxygen to form one of three isotopologues of water:

$$O_{ads} + 2H_{ads} \rightarrow H_2O\ (g) \tag{5.1a}$$

$$O_{ads} + 2D_{ads} \rightarrow D_2O\ (g) \tag{5.1b}$$

$$O_{ads} + H_{ads} + D_{ads} \rightarrow HDO\ (g) \tag{5.1c}$$

or scramble to recombinatively desorb as one of three isotopologues of dihydrogen:

$$2H_{ads} \rightarrow H_2\ (g) \tag{5.2a}$$

$$2D_{ads} \rightarrow D_2\ (g) \tag{5.2b}$$

$$H_{ads} + D_{ads} \rightarrow HD\ (g) \tag{5.2c}$$

Due to the molecular beam sizes, reaction 5.2 occurs in both area 1 and 2 (see figure 5.1), while reaction 5.1 only takes place in area 1. This is

confirmed by deconvoluting the HD signal in appendix D, showing that reaction 5.2 indeed only occurs in area 1 upon complete removal of O_{ads}. Similar behavior was observed previously for Pt(1 1 1).[104] Henceforth, we shall only consider reactivity by area 1. Further experimental details are provided in appendix D. The O_2 and HD signals yield direct and indirect evidence of the surface reactions at play:

$$R_{H_2O} \propto \frac{dP_{\mathrm{H_2O}}}{dt} \propto -\frac{1}{2}\frac{dP_{\mathrm{O_2}}}{dt} \propto -\frac{dP_{\mathrm{H_2}}}{dt} \tag{5.3}$$

where R is the reaction rate.

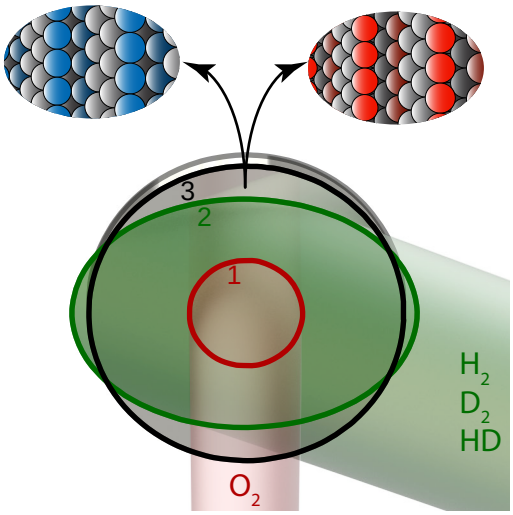

Figure 5.1: Schematic overview of the experiment. Area 1 of the surface is precovered with the supersonic O_2 beam (red), and the effusive H_2/D_2 beam (green) subsequently reacts with the adsorbed oxygen. Area 2 comprises the surface that is impinged by the effusive beam but is not precovered with O_{ads}. Area 3 is not impinged directly by either beam. Experiments are performed on Pt(3 3 5) (left) and Pt(5 5 3) (right) surfaces at a surface temperature of 500 K.

Results and Discussion

Figure 5.2 shows signal-averaged time-dependent O_2 sticking for the Pt(3 3 5) and Pt(5 5 3) surfaces, as measured using the King and Wells

method.[11] This is a pure room temperature expansion of O_2. The fit to the time of flight can be found in appendix D. The sticking behavior is representative of dissociative adsorption of O_2 on stepped Pt surfaces.[27, 101, 102] The O_2 sticking probability quickly drops over time as the O_{ads} coverage (θ_O) increases. Hence, O_2 sticking probabilities for both stepped surfaces are sensitive to coverage. Initial sticking probabilities (S_0) are extracted by fitting the data with a double exponential fit and extrapolating to the beam flag opening at t = 0.[27, 102] With sticking probabilities of 0.35 and 0.25, S_0 for Pt(5 5 3) exceeds that of Pt(3 3 5) under these conditions (T_s = 500 K, E_{kin} = 82 meV). Sticking on Pt(5 5 3) agrees well with previous results for low E_{kin} at T_s = 500 K.[102] Sticking at Pt(3 3 5) appears somewhat lower, which may be a result of a difference in E_{kin} distribution with previous results.[101]

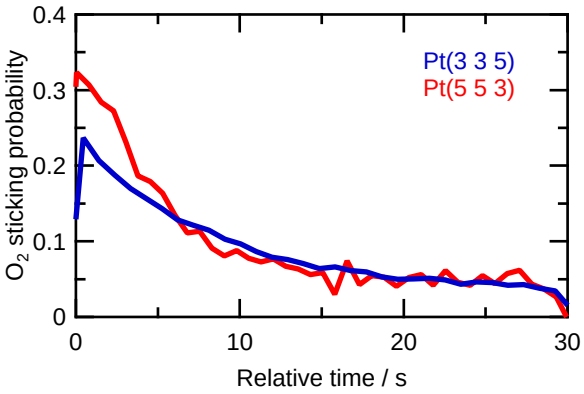

Figure 5.2: O_2 time-dependent sticking traces for the clean Pt(3 3 5) (blue) and Pt(5 5 3) (red).

Figure 5.3 shows the reactivity of area 1 for Pt(3 3 5) (left) and Pt(5 5 3) (right) as a function of time (horizontal axis), and O:H ratio in the zero coverage limit (vertical axis). Panels a and b show the change in O_2 sticking probability, whereas panels c and d report water formation measured through the variation in HD production. Attached to the four panels are O_2 sticking and R_{H_2O} curves exemplifying low (both) and high (R_{H_2O}) O:H ra-

tios. We explain the relation between water formation and HD production before discussing the results.

Dissociative adsorption of O_2, H_2, and D_2 leaves O_{ads}, H_{ads}, and D_{ads} on the surface. Our experiment is insensitive to recombinative desorption of $2H_{ads}$ and $2D_{ads}$ forming H_2 and D_2.[11] Only H_{ads} and D_{ads} that end up forming HD or water do not return as H_2 and D_2. Hence, the measured total reaction rate (R_{total}) results from H_{ads} and D_{ads} reacting to form either HD or a water isotopologue. We split the total reactivity into reactivity along equation 5.1 (R_{H_2O}) and equation 5.2 (R_{HD}). R_{HD} is equal to $2{\cdot}R_{H_2}$ and $2{\cdot}R_{D_2}$, assuming no isotope effect and isotropic mixing of H and D atoms. Chapter 4 shows this to be the case for (1 1 1), but not for (3 3 5) and (5 5 3). However, R_{HD} is then still proportional to the total rate of recombinative desorption of H_2, D_2, and HD.

We assume the same for water formation. R_{HDO} reflects water formation for all isotopes. When normalizing the total rate, recombinative desorption rate, and water production rate ($\hat{R}$), we may state:

$$\hat{R}_{HD} + \hat{R}_{H_2O} = 1 \tag{5.4}$$

Therefore, changes in $\hat{R}_{HD}$ directly reflect the change in $\hat{R}_{H_2O}$ by

$$\hat{R}_{H_2O} = 1 - \hat{R}_{HD} \tag{5.5}$$

In other words, H and D atoms not returning as H_2 or D_2 must have reacted to form either HD or an isotopologue of water. We normalize HD production by considering that HD production is maximized when area 1 is completely depleted of O_{ads}.

At 0 s in figure 5.3, the combination of the two beams initiates water formation via reaction 5.1. Panels a and b show that O_2 sticking gradually increases over time for both Pt(3 3 5) and Pt(5 5 3) upon impinging the hydrogen beam. For low hydrogen flux, O_2 sticking increases only to approximately 0.02. In contrast, O_2 sticking reaches 0.25 and 0.35 for Pt(3 3 5) and Pt(5 5 3) within 5 s, as illustrated by the two example traces. O_2 sticking is consistently higher for Pt(5 5 3) than Pt(3 3 5).

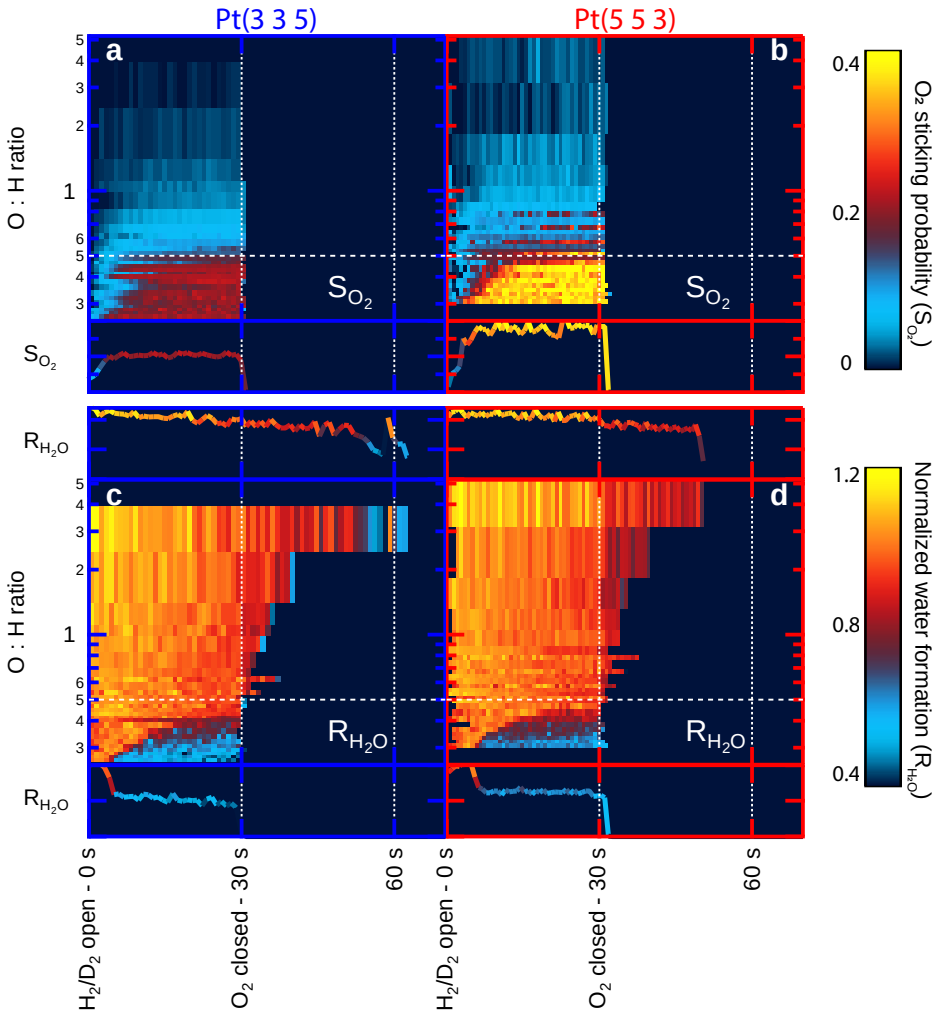

Figure 5.3: Comparison of O_2 sticking (top panels) and normalized water formation (bottom panels), R_{H_2O}, for Pt(3 3 5) (blue axes) and Pt(5 5 3) (red axes) measured as a function of time (bottom axes) and O:H ratio available for reaction at the clean surface (left axes). Normalized water production in panels c and d are extracted from HD formation (see text). At 30 s, the O_2 beam is discontinued. Shown for clarity are the O_2 sticking and R_{H_2O} traces for the lowest O:H ratio and the R_{H_2O} traces for the highest O:H ratio.

Panels c and d show that all initial hydrogen dissociation in area 1 of figure 5.1 leads to reaction 5.1. The data suggest that a rather constant flux of water forms for some time. Water formation occurs until 50 s for Pt(5 5 3) and well past 60 s for Pt(3 3 5) for hydrogen poor experiments, as exemplified by the top panels. With increasing hydrogen, the quick drop in water formation occurs earlier and converges to 30 s, i.e. where the incident O_2 flux is stopped.

The nearly constant water formation implies that most adsorbed hydrogen, which may potentially form HD by reaction 5.2, is consumed instead by reaction 5.1. An additional increase in $\hat{R}_{HD}$ reveals a drop in $\hat{R}_{H_2O}$ prior to 30 s if the hydrogen flux is sufficiently high. This behavior is exemplified by the two lower $\hat{R}_{H_2O}$ panels. There, in contrast to the constant initial $\hat{R}_{H_2O}$ observed for low hydrogen flux, a fraction of hydrogen ends up in reaction 5.2. Note that simultaneous to this drop in HD consumption, O_2 sticking in the top panels approximates S_0. Therefore, a steady state sets in upon complete O_{ads} removal, where reaction 5.1 becomes O_{ads} limited. As discussed previously, remaining hydrogen undergoes reaction 5.2. Appendix D details how we extract the O:H ratio from the O_{ads} limited data and extrapolate the O:H ratio to excess oxygen data.

We now compare how the time required to deplete the surface of O_{ads} depends on the O:H ratio for the two stepped surfaces. Figure 5.3 shows that the O_2 sticking probability increases as O_{ads} is removed with both time and H flux. Figure 5.4 shows the time required to remove all adsorbed oxygen from the surface as a function of the O:H ratio. Essentially, it follows the transition from orange to red/blue in $\hat{R}_{H_2O}$ in figure 5.3. Less time is required to remove all O_{ads} for Pt(5 5 3) (red) than Pt(3 3 5) (blue). The data show two linear regimes. Under oxygen lean conditions, approximately 5 s are required to remove all O_{ads} from O_{ads} buildup prior to impinging the hydrogen beam. As the relative amount of oxygen increases, so too does the time required to deplete the surface of O_{ads}. For O:H ratios approaching 0.5, approximately 30 s is required to consume all O_{ads}. At 30 s, the incident O_2 beam is discontinued and O_{ads} is no longer replenished

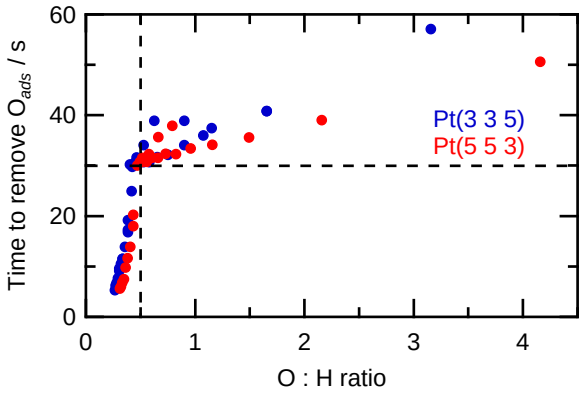

Figure 5.4: Reaction time required to remove all O_{ads} as a function of the oxygen-hydrogen ratio (see text) for Pt(3 3 5) (blue) and Pt(5 5 3) (red).

by the molecular beam. Consequently, a second regime is observed with a diminished slope. There, the hydrogen beam titrates remaining O_{ads} from the surface.

Figure 5.5 shows O_2 sticking in steady state, just prior to discontinuing the O_2 beam. O_2 reactivity matches S_0 fairly well for both surface under oxygen-lean conditions. As the O:H ratio increases in excess of 0.5, O_2 sticking decreases.

The overall reactivity behavior presented here closely resembles that of earlier titration and Molecular Beam Relaxation Spectroscopy results on Pt(1 1 1).[98, 104] H_{ads} selectively reacts with O_{ads} present at the surface. Upon complete O_{ads} removal, a steady state sets in where any incident O_2 that dissociates is immediately removed by H_{ads}. Excess H_{ads} (and D_{ads}) undergoes recombinative desorption.

In spite of lower step density, Pt(5 5 3) exhibits higher reactivity than Pt(3 3 5) under oxygen lean conditions. Higher Pt(5 5 3) reactivity towards reaction 5.1 is twofold. First, O_2 sticking under oxygen-lean conditions matches S_0, which is significantly higher for Pt(5 5 3). Second, higher

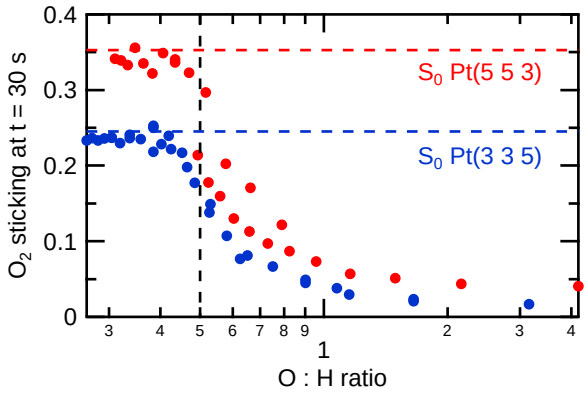

Figure 5.5: O_2 sticking prior to closing the O_2 flag at 240 s as a function of the oxygen:hydrogen ratio (see text) for Pt(3 3 5) (blue) and Pt(5 5 3) (red).

probabilities for O_2 sticking on Pt(5 5 3) than Pt(3 3 5) are incorporated in the O:H ratio, yet Pt(5 5 3) is depleted of O_{ads} faster than Pt(3 3 5). This suggests more hydrogen is available at the surface to react with O_{ads} to form water. Sticking of H_2 on O-covered Pt(3 3 5) is lower than the clean surface.[104, 105] This site blocking effect may be smaller for B-type steps, but requires further investigation beyond the scope of this study. Clearly, reactivity is structure sensitive.

The similarity of sticking under oxygen lean conditions and initial sticking at the clean surface suggests that little to no O_{ads} remains behind at the surface. It seems unlikely that a step edge with subsurface oxygen[98] is the active site, although we cannot completely rule this out. Our results clearly show that defect type is an important consideration in reactivity studies. Such details are currently lacking in the model for Pt(1 1 1) and results in a more complete description of reactivity at Pt surfaces.

Use of a supersonic molecular O_2 beam calls into question how our results compare to catalysis under realistic conditions. The subset of molecules present in our pure O_2 beam are certainly available under reaction conditions. However, the narrow energy distribution of our beam necessi-

tate further study considering the energy dependence of the reaction. For example, Pt(5 5 3) is more reactive towards O_2 dissociation in the present study at lower E_{kin}, but Pt(3 3 5) becomes significantly more reactive at higher kinetic energy.[101, 102]

Two other issues presented in the Pt(1 1 1) model remain unresolved. First, the model[98] proposes that all water forms at defects. Rate limiting O_{ads} diffusion towards defects cannot be identified from our results. Our experiments lack the temporal resolution of the Pt(1 1 1) experiments and the use of Pt(3 3 5) and Pt(5 5 3) single crystals does not allow variation of the step density. Second, the nature of the active site for oxygen reduction remains unresolved. Verheij[98] suggests kinks or oxygen-modified step edges may be responsible. Both issues may be resolved by adapting our apparatus that has combined molecular beam studies (this chapter) and tunable defect density of curved single crystals[27, 79](chapters 3 and 4), to also accommodate scattering experiments. In this manner, Molecular Beam Relaxation Spectroscopy may be performed as a function of A- and B-type defect density, extracting rate limiting O_{ads} diffusion[98]. By using two different curved Pt(1 1 1) samples – one with A- and B-type steps, the other with kinked surfaces – site-specific effective rate constants may be extracted for the three types of sites. This would unequivocally resolve the nature of the active site and how A-type, B-type, and kink density affects the effective rate constant.

Conclusion

In conclusion, we measured oxygen reduction reactivity for Pt(3 3 5) and Pt(5 5 3) using two molecular beams. Our results show that step type impacts reactivity, with higher reactivity for B-type steps on Pt(5 5 3) than A-type steps on Pt(3 3 5). These results highlight the importance of considering every possible reaction site available at the surface. Future studies should focus on the effect of step type and kinks on O_{ads} diffusion, the effective rate constant, and overall reactivity.